Atmos. Meas. Tech. Discuss., 7, 3349–3395, 2014
www.atmos-meas-tech-discuss.net/7/3349/2014/
doi:10.5194/amtd-7-3349-2014

Atmospheric Measurement Techniques Discussions
Open Access

A neural network approach for the simultaneous retrieval of volcanic ash parameters and SO_2 using MODIS data

A. Piscini[1], M. Picchiani[2], M. Chini[3], S. Corradini[1], L. Merucci[1], F. Del Frate[2], and S. Stramondo[1]

[1]Istituto Nazionale di Geofisica e Vulcanologia, Rome, Italy
[2]Earth Observation Laboratory, D.I.C.I.I. – Tor Vergata University, Rome, Italy
[3]Centre de Recherche Public – Gabriel Lippmann, Belvaux, Luxembourg

Received: 20 February 2014 – Accepted: 23 March 2014 – Published: 4 April 2014

Correspondence to: A. Piscini (alessandro.piscini@ingv.it)

Published by Copernicus Publications on behalf of the European Geosciences Union.

Abstract

In this work neural networks have been used for the retrieval of volcanic ash and SO_2 parameters based on Moderate Resolution Imaging Spectroradiometer (MODIS) multispectral measurements. Different neural networks were built for each parameter to be retrieved, experimenting different topologies and evaluating their performances.

As test case the May 2010 Eyjafjallajokull eruption has been considered. A set of six MODIS images have been used for the training and validation phases.

In order to estimate of the parameters associated with volcanic eruption such as ash mass, effective radius, aerosol optical depth and sulphur dioxide columnar abundance, the neural networks have been trained by using the retrievals obtained from well known algorithms based on simulated radiances at the top of the atmosphere estimated from radiative transfer models.

Three neural network's topologies with a different number of inputs have been compared: (a) only three MODIS TIR channels, (b) all multispectral MODIS channels and (c) only the channels that were selected by a pruning procedure applied to all MODIS channels.

Results show that the neural network approach is able to reproduce very well the results obtained from the standard algorithms for all retrieved parameters, showing a root mean square error (RMSE) computed from the validation sets below the target data standard deviation (STD).

In particular the network built considering all the MODIS channels gives a better performance in terms of specialization, mainly on images close in time to the training ones, while, as expected, the networks with less inputs reveals a better generalization performance when applied to independent datasets. In order to increase the network generalization capability, a pruning algorithm has been also implemented. Such a procedure permits to operate a features selection, extracting only the most significant MODIS channels from images. The results of pruning revealed that obtained inputs,

AMTD

7, 3349–3395, 2014

for all the retrieved parameters, correspond to the TIR channels sensitive to ash, plus some other channels in the visible and mid-infrared spectral ranges.

The artificial neural network approach proved to be effective in addressing the inversion problem for the estimation of volcanic ash and SO_2 cloud parameters, providing fast and reliable retrievals, which are important requirements during the volcanic crisis.

1 Introduction

The Eyjafjallajokull volcanic eruption occurred in Iceland between April and May 2010 revealing once more the importance of the effects produced by this natural hazard (Zehner, 2010) and demonstrated how much a reliable real time monitoring and tracking of volcanic clouds is crucial. In particular the volcanic ash affects climate (Robock, 2000), human safety (Horwell and Baxter, 2006) and represents a severe threat to aviation (Miller and Casadevall, 2000). Furthermore SO_2 is considered as volcanic ash proxy when this latter is undetectable, it has long term effects on aircraft engines and covers an important role in volcanic processes (Allard et al., 1994; Wallace, 2001; Edmonds et al., 2010).

Although the ash detection algorithm is quite fast, the well-known methods used for the simultaneous quantitative estimation of ash and SO_2, based on comparison between top of atmosphere (TOA) radiance with the simulated one obtained using a radiative transfer model, need a high computational time and many parameters as input (see Sect. 3 for details). These reasons make the real time application of the standard retrieval procedures difficult during the volcanic crisis.

The Neural Network (NN) approach has demonstrated its effectiveness in geophysics, because NN represents a *universal approximator*, being able to model physical nonlinear phenomena and to solve complex inversion problems (Krasnopolsky et al., 1995). Furthermore its strength is represented by a very low computation time required during application phase, so that the computational burden required for the data processing is drastically reduced. This characteristic assumes an important role when considering the possible application to really high revisit time sensors like Meteosat Second Generation (MSG) SEVIRI.

In the remote sensing of atmosphere the NNs have been successfully applied in order to address different problems such as: height resolved ozone retrievals (Del Frate et al., 2002; Müller et al., 2003; Sellitto et al., 2011), retrieval of temperature profiles (Churnside et al., 1994; Del Frate and Schiavon, 1999), cloud classification (Lee et al., 1990; Bankert, 1994), temperature estimations (Butler et al., 1996) and humidity profiles retrieval (Cabrera-Mercader and Staelin, 1995; Del Frate and Schiavon, 1999; Blackwell, 2005). Furthermore in Gardner and Dorling (1998) and Hsieh and Tang (1998) has been demonstrated how NNs can resolve inverse problems involving complex physical behaviors.

Recently, NNs have been also applied to the detection of ash plume and the retrieval of the ash mass on Etna volcano scenario, using a topology involving channels centered at 11 µm and 12 µm plus the water vapor absorption at 7.3 µm (Picchiani et al., 2011). In such study the retrieval was conducted only above the sea, since the scenario did not imply the presence of ash and meteorological clouds on the same pixels. In Picchiani et al. (2012a) the procedure was extended to completely characterize the set of ash parameters showing some preliminary analysis of a more complex scenario such as the Eyjafjallajokull volcano.

In this study NNs have been used for retrieving ash total mass, particle effective radius (r_{eff}), Aerosol Optical Depth (AOD) at 11 µm and SO_2 at 8.7 µm total column abundance from MODIS images. To this aim the comparison between different input network topologies, also making use of the pruning as a feature selection technique, has been performed in order to find the most significant inputs and increase the retrieval performances. Furthermore, since the performance of neural network is strictly related to reliability of training samples used, the reference data set has been selected considering two different scenarios: volcanic clouds over the sea and volcanic clouds over meteorological clouds (see Sect. 3.2 for details). For both cases the standard retrieval strategy has been adopted, except for the underlying surface temperature that

AMTD
7, 3349–3395, 2014

in the first case is the sea surface temperature and in the second case is the meteorological cloud top temperature (Corradini et al., 2010).

The work is organized as follows. We first provide an overview of the considered scenario, discussing the MODIS sensor characteristics as well (Sect. 2), then we discuss and discuss the basic concepts of ash and SO_2 parameters retrievals (Sect. 3). In section four the NNs approach is introduced while in section five the methodology s described. Finally the results are discussed (Sect. 6) and the conclusions reported (Sect. 7).

2 Test case description – the Eyjafjallajokull eruption

Eyjafjallajökull volcano (lat: 63.63° N, long: 19.62° W) is a 1666 m high stratovolcano with a 2.5 km wide summit caldera located on the south of Iceland. Although the Eyjafjallajökull erupted during historical time, it has been less active than other volcanoes of Iceland's eastern volcanic zone (Smithsonian Institution, Volcanism Global Program). A significant eruption at Eyjafjallajokull took place in 1821 and featured intermittent explosive events that deposited a thin tephra layer on the flanks of the volcano over a period of about 18 months.

The explosive activity occurred from 14 April to 23 May 2010 caused widespread disruption to aviation and with an enormous impact on the world economy. This eruption may be considered the biggest explosive eruption in Iceland since that of Hekla occured in 1947 (Zehner, 2010).

Following an intense seismic swarm the eruption began from the summit of the Eyjafjallajokull volcano at 01:15 UTC on 14 April 2010. Initially the activity was subglacial but around 06:00 UTC a white (steam-rich) eruption plume rose from the summit (Sigmundsson et al., 2010).

Three different eruption phases were observed (Zenher, 2010):

AMTD
7, 3349–3395, 2014

– a sustained phreatomagmatic eruption occurred from 14 to 17 April with production of a large amount of fine ash of trachyandesite composition with a 5–9 km-high volcanic ash (Gudmundsson et al., 2010). Prevailing winds carried the ash-rich eruption plume towards southeast and south and thereafter over Europe;

– from 18 April to 4 May a marked change in style and intensity of the eruption was registered although the composition of the erupted magma was unchanged. The eruption style changed from phreatomagmatic to magmatic, implying that external water no longer had ready access to the vents. During this phase, the explosive activity decreased by an order of magnitude than the previous phreatomagmatic one with a reduction in ash emission with a plume height between 2 and 5 km (a.s.l.);

– from 5 to 23 May the eruption style changes to explosive. Following an episode of renewed seismic activity, Eyjafjallajokull volcano started a new phase with a come back to the previous magmatic phases with a more ash production. The intensity of explosive activity increased again and observations reported volcanic ash heights around 4–6 km, sometimes reaching up to 8–9 km. This resurgence in activity led to further disruption to air traffic in Europe.

In this work, we have concentrated our attention on the last eruption phase, by considering six MODIS images collected between 6 May, and 13 May 2010.

MODIS is a multi-spectral instrument aboard on the Earth Observing System (EOS) Terra and Aqua satellites (Barnes et al., 1998; http://modis.gsfc.nasa.gov/). The two satellites have different equatorial crossing times: Terra is characterized by a morning overpass, while Aqua by an afternoon one, with a global coverage in 1 or 2 days. MODIS covers 36 spectral bands, from visible (VIS) to Thermal Infrared (TIR), and a spatial resolution that varies from 250 m to 1000 m, depending on the acquisition mode.

AMTD
7, 3349–3395, 2014

3 Ash and SO_2 retrievals

In this Section the standard ash and SO_2 retrieval procedures applied to the MODIS measurements in the TIR will be briefly described. The TIR channels characteristics are given in Table 1. The products obtained have been used as target output for NNs training and as "ground truth" in the validation phases.

3.1 Ash detection and retrievals

The most widely adopted approach to detect volcanic ash, and to discriminate it from meteorological clouds, is based on the different spectral absorption of ash and water vapor/ice particles between 11–12 µm. The difference between the brightness temperature (BTD) computed from two channels centered around 11 ($T_{b,11}$) and 12 µm ($T_{b,12}$) is generally negative for volcanic ash and positive for meteorological clouds (Prata, 1989a). The ash r_{eff} and AOD are retrieved by computing the inverted arches curves BTD-$T_{b,11}$ using radiative transfer models, while the ash mass is estimated using the simplified formula introduced by Wen and Rose in 1994 (Wen and Rose, 1994; Yu et al., 2002). The BTD method has been applied to satellite instrument measurements as the Advanced Very High Resolution Radiometer (AVHRR) (Prata, 1989b; Wen and Rose, 1994; Corradini et al., 2010), MODIS (Hillger et al., 2002; Watson et al., 2004; Tupper at al., 2004; Corradini et al., 2008, 2010, 2011), the Geostationary Operational Environmental Satellite (GOES) (Yu et al., 2002), and the Spin Enhanced Visible and Infrared Imager (SEVIRI) measurements (Prata and Kerkmann, 2007; Corradini et al., 2009).

The simulated Top of Atmosphere (TOA) radiances Look-Up Table (LUT) necessary for the retrievals are computed using the MODTRAN 4 (Berk et al., 1989; Anderson et al., 1995) Radiative Transfer Model (RTM) (Corradini et al., 2009, 2010, 2011) using the Keflavikurflugvollur (lat: 63.95°, long: −22.60°) WMO atmospheric profiles (PTH) and andesitic ash optical properties (Pollack, 1973).

AMTD
7, 3349–3395, 2014

3.2 SO_2 retrieval

The SO_2 retrieval in the TIR spectral range is realized by exploiting its wide absorption around 8.7 µm (MODIS channel 29). The retrieval scheme derived from Realmuto et al. (1994, 1997) was initially applied to the Thermal Infrared Multispectral Scanner (TIMS) measurements, and later on was successfully extended to several space-based sensors such as MODIS (Watson et al., 1994; Corradini et al., 2009, 2010), Advanced Spaceborne Thermal Emission and Reflection Radiometer (ASTER) (Corradini et al., 2004; Pugnaghi et al., 2006) and SEVIRI (Corradini et al., 2009). The algorithm is based on a weighted least square fit procedure between the simulated radiances obtained by varying the SO_2 columnar amount with MODTRAN RTM and the sensor radiances measured. The 8.7 µm band lies in the thermal infrared atmospheric window which is relatively transparent to water vapor and therefore generally used for the tropospheric volcanic clouds retrievals. Limitations to the applicability of this retrieval scheme are due to a lower thermal contrast between the SO_2 cloud and the underlying surface, and opaque pixels, i.e. pixels where the minimum simulated radiance exceeds the TOA radiance measured by the sensor. A relevant improvement has been proposed by Corradini et al. (2009) to take into account the interference due to the ash presence in the volcanic plume. Since ash and SO_2 are often ejected simultaneously during volcanic eruptions and volcanic ash absorbs in the same 8.7 µm band, the SO_2 abundance can be highly overestimated if the ash contribution to the TOA radiance is neglected. The ash correction on SO_2 retrieval has been recently validated by comparing the SO_2 flux extract from a MODIS image and the flux measured by the FLux Automatic MEasurements (FLAME) ground-based network (Salerno et al., 2009) deployed at Mt. Etna, Sicily (Merucci et al., 2011). The SO_2 maps presented here are corrected for the ash cloud content and have been retrieved by means of custom procedures described in detail on Corradini et al. (2009). Among the different source of ash and SO_2 retrieval errors deriving from the uncertainties on RTM input parameters (Corradini et al., 2008, 2009), the non-uniformity of the surface underlying the volcanic

AMTD
7, 3349–3395, 2014

cloud is one of the most critical. Such a condition is common when the volcanic cloud is wide enough to insist in a region in which a partial meteorological clouds cover is present. In these cases the retrievals have to be realized by considering different surface temperatures for the different volcanic cloud parts insisting over different surfaces (land, sea or meteorological clouds). For the case study considered in this work the surfaces under the volcanic cloud are sea and meteorological clouds (see Fig. 1). The sea surface temperature is computed by a standard procedure based on the inversion of the radiative transfer equation in the TIR spectral range (Corradini et al., 2008) while the surface temperature of the meteorological cloud has been estimated by computing the brightness temperature at 11 µm (MODIS channel 31). This latter approximation is all the more valid for high and opaque meteorological clouds. In this case the retrieval accuracy is lower than the achieved by considering a volcanic cloud over a sea surface because of the lower thermal contrast between meteorological cloud top surface and ash cloud temperature (Watson et al., 2004). The above procedure was carried out in order to increase the accuracy of retrievals used for neural network training phase.

In this work the ash parameters and SO_2 retrievals estimated with the methodology described in Corradini et al. (2009, 2010) have been used for NNs training and validation.

4 Neural Netwoks

Since the 1990s NNs have been applied in many remote sensing fields (Atkinson and Tatnall, 1997; Mas and Flores, 2008) including significant atmospheric investigation (Gardner and Dorling, 1998). The increased interest in the management of remote sensing data by this technique can be understood considering the universal approximation property of the most common type of NN, such as the Multi-Layer Perceptron (MLP). The theorem, proved by Cybenko (1989), explains as a MLP with a single hidden layer, which contains finite number of neurons with sigmoidal activation function, is an universal approximator among continuous functions on compact subsets of $\underline{R}^n$.

Further attractions are the independence from a priori assumptions about the statistical characterization of the data and the possibility to easily incorporate different type of data (Foody, 1995). For these reasons NNs have been often successfully used for the solution of the inverse problem of geophysical quantities from satellite measurements (Blackwell, 2005; Sellitto et al., 2011; Picchiani et al., 2012b).

The architecture of a MLP is based on a simple processing unit, called neuron, which collects the quantities presented in input, through weighted connections, and produces the output applying an activation function to the weighted sum of the inputs. The neurons are interconnected and organized in at least three layers, one input layer, a variable number of intermediate hidden layers and one output layer. The first layer distributes the data, without processing it, to all neurons in the first hidden layer, then the information is passed to the second hidden layer and so on up to the output layer.

For remote sensing applications, usually, the input layer collects values in the form of Digital Numbers (DNs), e.g. radiances or brightness temperatures, from spectral bands through a number of nodes equals to the number of bands. Therefore each input pattern represents the spectral signature of the respective pixel of the image. The output layer produces the retrieved geophysical parameter value corresponding to the specific input. In this work we used the same approach developed in Picchiani et al. (2011) to train the NNs. The back-propagation algorithm (Bishop, 1995) has been applied performing a cross-validation approach (Haykin, 1994; Bishop, 1995) to avoid the over training insurgence (i.e. the memorization of patterns trends instead of the statistical mapping linking the inputs to outputs), that could vanish the generalization capability on new data. In this phase two data sets called training and test have been respectively used to change the weights and to stop the training algorithm before the generalization capability started decreasing.

To assess the network performance of the trained net, a third independent data set (validation set) is usually used. Indeed, many different settings influence the ability of an NN to generalize. Among the most important ones we have the network topology, i.e. the number of hidden layers and of neurons in each layer, the number of training

Discussion Paper | Discussion Paper | Discussion Paper | Discussion Paper |

AMTD

7, 3349–3395, 2014

Monitoring of volcanic ash and SO_2 from MODIS using Neural Networks

A. Piscini et al.

epochs and the number of inputs. Concerning the latter aspects, a feature selection approach, aiming at selecting a subset of the inputs relevant for a given retrieval problem, could be very effective in this framework. Its two main purposes are, to speed up the learning process, since the amount of data to be processed is reduced, and to give the possibility to empirically discover which are the most effective spectral wavelengths for the particular retrieval problem.

A well-known features selection technique using NNs is the pruning, which is generally aimed at training a network larger than necessary and then at pruning the neurons and the connections that are not needed, i.e. the elements showing low influence on the network's result. In this way also the inputs node may be pruned, so the algorithm acts as a features selector (Pacifici et al., 2009), searching for the wavelengths having major correlation with the geophysical parameter in output. After the training phase, the units (the network neurons) are analyzed to determine those not contributing significantly to the solution. This phase is the most important one in the procedure implementation and it guides the weights suppression. The relative importance, or saliency, of different weights is the measure, generally adopted, to judge if a node will be removed. This is defined as the sum of weights afferent to the neuron, i.e. less important weights have smaller saliencies.

Within different pruning algorithms we chose the Optimal Brain Surgeon (OBS) (Stork and Hassibi, 1993), which is capable to give good results in terms of accuracy and stability, despite its higher computational effort due the computation of the inverse of the Hesse-Matrix to deduce saliency and weight change for every link. There are two criteria to stop the pruning, the error after each retraining must not exceed the error before the first training more than a certain percentage, or the error after each retraining must not exceed a given absolute error value.

The first approach allowed us a more effective selection of the inputs and a reduction of the error with respect to the performance of the all-units network initially obtained.

AMTD
7, 3349–3395, 2014

5 Methodology

The main objective of the work is to retrieve the three volcanic ash related parameters and SO_2 total columnar amount by means of NNs, having as a benchmark the MODTRAN based results, but also to study which are the most effective wavelengths to successfully reach the fixed target. To this aim three different NNs have been implemented considering different set of inputs to exploit both the model approach (i.e. TIR channels) and the full sensor capability. The three NNs are: NN-3 which uses the three channels exploited in the physical model; NN-ALL which makes use of all bands provided by MODIS sensors; NN-P which uses the bands selected by the pruning algorithm starting from the all available channels. Using the NN-3 to retrieve the three ash parameters three MODIS thermal channels, 31 and 32 and 28, have been used as suggested by BTD model, where the channel 28 takes into account the water vapor absorption. For the SO_2 retrieval, the channel 29 centered at 8.7 µm has been used instead of the 28.

Even if the systematic identification of the best topology is out of the scope of this study, we have performed a trial an error step to select the best architecture. The optimization step has been done for NN-3 and NN-ALL, and it was mostly focused to find the best topology for the hidden layers, while the input one is fixed by the number of bands. Both optimization processes have provided the same topology for NN-3 and NN-ALL, one hidden layer of 15 neurons, thus we extended this result to the NN-P, which is completely retrained after the pruning step, using only the selected inputs. In order to focus on the selection of the most significant MODIS channels the pruning procedure has been applied disabling the possibility to change the NN hidden layers topology. In this way the pruning procedure has been only used as feature selection tool.

For the study we collected six MODIS images related to third phase of Eyjafjallajokull eruption, from 6 May 2010 to 13 May 2010 (see Fig. 1). Therefore the MODTRAN standard procedures has been used to extract the SO_2 and the three ash parameters for all available images.

Since the back-propagation training algorithm is supervised some examples of the phenomena under investigation are needed. To this aim the results of the MODTRAN based inversion have been considered as target output during the training phase. The whole set of MODIS acquisitions (Fig. 2) has been split in two parts: four dates for the training phase (6, 7, 8 and 13 May), and the remaining two dates as an independent validation set (11, 12 May). This approach has been taken into account for assessing the generalization capabilities of the NNs and the statistical significance of the training and test samples. The NNs retrieval has been focused on the regions in images affected by ash plume, according to the BTD ash maps, indifferently of the presence of only ash or ash cloud mixed with meteorological clouds. It is worth noticing that the NNs retrieval approach has been applied in a real scenario, where meteorological clouds are present as well, introducing additional difficulties in the parameters estimation. Indeed in the MODTRAN based scheme, the retrieval of all these parameters in such condition increases the difficulties on parameterizing the model itself. In particular, the NNs training uses pixels from an overlap of meteorological and ash clouds, and pixels from volcanic ash above the sea, without disjointing the retrieval problem, while the MODTRAN based approach has to treat separately the two cases.

For each date of the training dataset, three distinct subsets have been created, such as Training, Test and a Validation sets, and they are summarized in Tables 2 and 3, while the two validation dates are shown in Tables 4 and 5. The independent validation pixels have been further split in sea and clouds, depending on where the ash plume were lying, in order to evaluate also the capability of the NNs to deal with these two distinct scenarios; whilst this differentiation has not been adopted for the training set since we want to retrieve parameters using a unique neural network.

AMTD
7, 3349–3395, 2014

6 Results and discussion

In this section the results obtained by applying the three NNs (NN-3, NN-ALL and NN-P) for the retrieval of the three ash cloud parameters and SO_2 are presented. First the NNs-based retrievals have been compared to results obtained by applying the classical approach, and then the performance of the NNs retrieval has been discussed.

With regard to the ash parameters the results are summarized in Tables 6–8. As a first general remark, the RMSE of all retrievals is lower than the corresponding STD for all NNs configurations (NN-3, NN-ALL and NN-P). This is an indication that the NNs are a valuable approach for this kind of problem. The second remark is that better results have been generally obtained with more inputs NNs, namely NN-ALL and NN-P. This second outcome could appear not in agreement with the results obtained by Picchiani et al. (2011) if we compare their results and the present ash mass retrievals. In Picchiani et al. (2011) it seemed that the performance obtained here with NN-ALL and NN–P, was already reached with a network based only on the three TIR channels. An explanation can be found considering the lower complexity of the scenario analyzed in the previous work where the overlapping of volcanic ash and meteorological clouds was not considered.

In Figs. 3–8 the scatter plots computed considering the two independent validation sets are shown, and the results of the three NNs topologies, i.e. NN-3, NN-ALL and NN-P are reported for each parameter.

As for the Tables, also the scatter plots for the two validation images have been divided in two regions, distinguishing the ash plume on sea from that on meteorological clouds, in order to evaluate the performances on the NNs in the two different scenarios. Looking at the scatter plots, the results confirm the findings obtained by Picchiani et al. (2011) for ash mass retrieved above sea, using the input selection based on physical considerations. Moreover they provide the effectiveness of the methodology for the other parameters and in a more complex physical scenario. The scatter plots also show a general agreement between the values obtained by the radiative transfer model inversion and the NNs ones. There is a certain degree of retrieval underestimation characterizing all parameters for both test dates. The patterns above meteorological clouds show a lower accuracy than the patterns above sea. The high error of NN inversions depends on the higher uncertainty of the standard retrieval procedure in case of the presence of a meteorological cloud due to the non homogeneity of the meteorological cloud itself. Moreover for the temperature on clouds top, the brightness temperature has been considered instead of the physical temperature. This approximation is more reasonable for higher clouds. A deeper comparison of NN-3 and NN-ALL outcomes shows that better performances above sea have been obtained when the spectral information increases (NN-ALL and NN-P).

As expected and confirmed by experimental results, the NN-ALL and NN-P provided almost the same results, since in the procedure to obtain the NN-P from the NN-ALL we tried to decrease the number of inputs without affecting the retrieval capabilities. In Table 9 all bands selected by the procedure are summarized. In this way the redundant information are neglected, allowing to train the network faster and to obtain a better generalization on independent test cases. Moreover, the pruning selection has always included the MODIS channels with the highest physical meaning, i.e. the channels 31 and 32. For all three parameters the pruning step selects around 50 % of the input space. As Table 9 shows, the most common MODIS channels selected by the pruning procedure applied to the different ash parameters are the channels 1, 3 and 4 sensitive to the very fine ash, 23 and 25 sensitive to cloud surface and atmospheric temperature respectively and the channels 36 sensitive to the cloud top altitude.

The NN-P maps (Figs. 11–13), representing the best results obtained for all three parameters, have been compared to the model based results for the two validation dates. Looking at the figures the good performance of the NN approach is confirmed for the three ash parameters, indeed the MODTRAN based and NN-P results show are in good accordance (i.e. colours) and shape features.

As regard to the SO_2, RMSE is still lower than STD of parameter distribution, even if it is higher with respect to the ash parameters, especially in the meteorological cloud

AMTD
7, 3349–3395, 2014

case (see Tables 6–8). Looking to scatter plots (Figs. 9 and 10), if we focus our attention only on the SO_2 above the sea, results are better if we increase the number of inputs, while with the meteorological cloud some problems are present. Indeed the retrieval above meteorological cloud is not satisfactory with NN-3, and it does not improve if we increase the number of inputs (Figs. 9 and 10, right column).

In Figs. 14 and 15 are reported the comparison between the model based and NN results maps. In these cases both NN-3 and NN-P results are shown to highlight as the pruning analysis does not improve the results obtained considering only three channels, in particular when plume laying above meteorological cloud (see Fig. 15). Nevertheless, looking at Fig. 14, where NN has been applied to validation date of 11 May 2010, the retrieval obtained by NN-P shows a higher accuracy than that obtained by NN-3.

The reason of the better NN ash retrieval performance and of the worst one in case of SO_2 retrieval when the addition of different MODIS channels is considered might be explained by the different selective interactions between the two species in the wavelengths from VIS to TIR. The aerosol particles, as volcanic ash, do not present a defined spectral signature at specific wavelengths, but they interact (with absorption and scattering) continuously overall the VIS-TIR spectral range. In this case the channels addition will increase, even if only slightly, the information content on the ash presence in the atmosphere. Conversely, SO_2 presents spectral signatures more sensitive to specific wavelengths, thus increasing the number of input channels outside the absorption signature will mainly increase the noise without improving the information content.

7 Conclusions

The NNs have been effective in solving the inversion problem related to the estimation of the volcanic cloud parameters, addressing the issue related to presence of false alarms in the detection of volcanic ash. Morevoere, after the training phase is

AMTD
7, 3349–3395, 2014

completed, NNs have confirmed to be a fast retrieval technique, very useful at application stage. From this point of view the technique satisfies the need to provide results quickly in case of disastrous natural events, such as volcanic eruptions.

Volcanic ash and SO_2 clouds were detected and characterized over sea and over meteorological clouds simultaneously. The results confirm the effectiveness of the approach especially considering the main goal of obtaining accurate retrieval for the plume above the sea. We have proved that the simplified topology obtained by considering only three input channels, is almost unable to describe the complexity of the considered scenario and that pruning analysis can be conveniently applied to find other significant input channels and improve NNs performance's accuracies.

Moreover, the increase of the number of inputs with other MODIS channels improves the ash retrieval over the sea, and provides appreciable results on patterns characterized by meteorological clouds. The retrieval accuracy over the sea is not compromised by the presence of meteorological clouds underlying the ash cloud in the training set. In fact it seems that the NNs approximate the main relationship between ash characteristics and radiometric measurement, despite of the presence of effects due to meteorological clouds. Especially for the ash parameters the majority of the validation pixels were properly retrieved in both the scenarios. The spread shown in the scatter plots, describing pixels above meteorological cloud, is due to some boundary effects on the region between plume and clouds. This behavior can be interpreted as a posteriori validation of the forward model accuracy over meteorological clouds, indeed it seems that the NNs address quite well the core of the plume on the cloud, where the forward model gives good results, and faults the retrieval of ash boundary pixels, characterized by mixed effects of ash and clouds, confirming the high uncertainty of forward model in describing such a complex scenario.

On the other hand, the pruning analysis was able to apply a feature selection of input data-set maintaining the significant inputs and improving or leaving unaltered the accuracy of NN.

AMTD
7, 3349–3395, 2014

Results obtained for SO_2 with the same approach are slighter worse, but in any case the pruning technique succeeds in finding the significant inputs improving the NN performance.

Future studies will include testing the usefulness of the technique under different light conditions (night-time) and on different multispectral remote sensed data, such as those provided by high revisit time sensors like MSG-SEVIRI, on board the METEOSAT Second Generation satellites. The last one would be particularly suitable for its extreme quick response that is a key property for real-time monitoring of the atmosphere.

Acknowledgements. Marco Chini's contribution was supported by the National Research Fund of Luxembourg through the PAPARAZZI project (CORE C11/SR/1277979).

References

Allard, P., Carbonnelle, J., Metrich, N., Loyer, H., and Zettwoog, P.: Sulphur output and magma degassing budget of Stromboli volcano, Nature, 368, 326–330, 1994.

Anderson, G. P., Wang, J., and Chrtwynd, J. H.: MODTRAN3: An update and recent validation against airborne high resolution inferometer measurements, in: Summaries of the Fifth Annual Jet Propulsion Laboratory Airborne Earth Science Workshop, 95–1(1), 5–8, 1995.

Atkinson, P. M. and Tatnall, A. R. L.: Neural networks in remote sensing, Int. J. Remote Sens., 18, 699–709, 1997.

Bankert, R. L.: Cloud classification of AVHRR imagery in maritime regions using a probabilistic neural network, J. Appl. Meteorol., 33, 909–918, 1994.

Barnes, W. L., Pagano, T. S., and Salomonson, V. V.: Prelaunch characteristics of the Moderate Resolution Imaging Spectroradiometer (MODIS) on EOS-AMI, IEEE T. Geosci. Remote, 36, 1088–1100, 1998.

Berk, A., Bernstein, L. S., and Robertson, D. C.: MODTRAN: a Moderate Resolution Model for LOWTRAN, 7, 1989.

Bishop, C. M.: Neural Networks for Pattern Recognition, Oxford University Press, 1995.

Blackwell, W. J.: A neural-network technique for the retrieval of atmospheric temperature and moisture profiles from high spectral resolution sounding data, IEEE T. Geosci. Remote, 43, 2535–2546, 2005.

Butler, C. T., Meredith, R. V. Z., and Stogryn, A. P.: Retrieving atmospheric temperature parameters from DMSP SSM/T-1 data with a neural network, J. Geophys. Res., 101, 7075–7083, 1996.

Cabrera-Mercader, C. R. and Staelin, D. H.: Passive microwave relative humidity retrievals using feed forward neural networks, IEEE T. Geosci. Remote, 33, 1324–1328, 1995.

Churnside, J. H., Stermitz, T. A., and Schroeder, J. A.: Temperature profiling with neural network inversion of microwave radiometer data, J. Atmos. Ocean. Tech., 11, 105–109, 1994.

Corradini, S., Pugnaghi, S., Teggi, S., Buongiorno, M. F., and Bogliolo, M. P.: Will ASTER see Etna SO_2 plume?, Int. J. of Remote Sens., 24, 1207–1218, 2003.

Corradini, S., Spinetti, C., Carboni, E., Tirelli, C., Buongiorno, M. F., Pugnaghi, S., and Gangale, G.: Mt. Etna tropospheric ash retrieval and sensitivity analysis using Moderate Resolution Imaging Spectroradiometer measurements, J. Appl. Remote Sens., 2, 023550, doi:10.1117/1.3046674, 2008.

Corradini, S., Merucci, L., and Prata, A. J.: Retrieval of SO_2 from thermal infrared satellite measurements: correction procedures for the effects of volcanic ash, Atmos. Meas. Tech., 2, 177–191, doi:10.5194/amt-2-177-2009, 2009.

Corradini, S., Merucci, L., Prata, A. J., and Piscini, A.: Volcanic ash and SO_2 in the 2008 Kasatochi eruption: retrievals comparison from different IR satellite sensors, J. Geophys. Res., 115, D00L21, doi:10.1029/2009JD013634, 2010.

Corradini, S., Merucci, L., and Arnau, F.: Volcanic ash cloud properties: comparison between MODIS satellite retrievals and FALL3D transport model, IEEE Geosci. Remote S., 8, 248–252, 2011.

Cybenko, G.: Approximation by superpositions of a sigmoidal function, Math. Control Signal., 2, 303–314, 1989.

Del Frate, F. and Schiavon, G.: Nonlinear principal component analysis for the radiometric inversion of atmospheric profiles by using neural networks, IEEE T. Geosci. Remote, 37, 2335–2342, 1999.

Del Frate, F., Ortenzi, A., Casadio, S., and Zehner, C.: Application of neural algorithms for a real-time estimation of ozone profiles from GOME measurements, IEEE T. Geosci. Remote, 40, 2263–2270, 2002.

Del Frate, F., Iapaolo, M., Casadio, S., Godin-Beekmann, S., and Petitdidier, M.: Neural networks for the dimensionality reduction of GOME measurement vector in the estimation of ozone profiles, J. Quant. Spectrosc. Ra., 92, 275–291, 2005.

Edmonds, M., Aiuppa, A., Humphreys, M., Moretti, R., Giudice, G., Martin, R. S., Herd, R. A., and Christopher, T.: Excess volatiles supplied by mingling of mafic magma at an andesite arc volcano, Geochem. Geophy. Geosy., 11, Q04005, doi:10.1029/2009GC002781, 2010.
Foody, G. M.: Using prior knowledge in artificial neural network classification with a minimal training set, Int. J. Remote Sens., 16, 301–312, 1995.
Gardner, M. W. and Dorling, S. R.: Artificial neural networks (the multilayer perceptron) – a review of applications in the atmospheric sciences, Atmos. Environ., 32, 2627–2636, 1998.
Gudmundsson, M. T., Pedersen, R., Vogfjörd K., Thorbjarnardóttir B., Jakobsdóttir S. S., and Roberts, M. J.: Eruptions in Eyjafjallajökull Volcano, Iceland: EOS (Transaction American Geophysical Union), 91, 190–191, doi:10.1029/2010EO210002, 2010.
Haykin, S.: Neural Networks: a Comprehensive Foundation, Macmillan, New York, 1994.
Hagiwara, M.: Removal of hidden units and weights for backpropagation networks, in: Proc. IEEE Int. Joint Conf. Neural Netw., 351–354, 1993.
Hillger, D. W. and Clark, J. D.: Principal component image analysis of MODIS for volcanic ash, Part I: Most important bands and implications for future GOES imagers, J. Appl. Meteorol., 41, 985–1001, 2002.
Horwell, C. J. and Baxter, P. J.: The respiratory health hazards of volcanic ash: a review for volcanic risk mitigation, B. Volcanol., 69, 1–24, doi:10.1007/s00445-006-0052-y, 2006.
Hsieh, W. W. and Tang, B.: Applying neural network models to prediction and data analysis in meteorology and oceanography, B. Am. Meteorol. Soc., 79, 1855–1870, 1998.
Krasnopolsky, V. M., Breaker, L. C., and Gemmill, W. H.: A neural network as a nonlinear transfer function model for retrieving surface wind speeds from the special sensor microwave imager, J. Geophys. Res., 100, 11033–11045, 1995.
Lee, J., Weger, R. C., Sengupta, S. K., and Welch, R. M.: A neural network approach to cloud classification, IEEE T. Geosci. Remote, 28, 846–855, 1990.
Mas, J. F. and Flores, J. J.: The application of artificial neural networks to the analysis of remotely sensed data, Int. J. Remote Sens., 29, 617–663, 2008.
Merucci, L., Burton, M., Corradini, S., and Salerno, G. G.: Reconstruction of SO_2 flux emission chronology from space-based measurements, J. Volcanol. Geoth. Res., 206, 80–87, 2011.
Miller, T. P. and Casadevall, T. J.: Volcanic ash hazards to aviation, in: Encyclopedia of Volcanoes, edited by: Sigurdsson, H., Academic Press, San Diego, 915–930, 2000.

AMTD
7, 3349–3395, 2014

Monitoring of volcanic ash and SO_2 from MODIS using Neural Networks

A. Piscini et al.

Mozer, M. and Smolensky, P.: Skeletonization: a technique for trimming the fat from network via relevance assessment, in: Advances in Neural Information Processing Systems, edited by: Touretzky, D., vol. 1, Morgan Kaufmann, San Mateo, CA, 107–115, 1991.

Müller, M. D., Kaifel, A. K., Weber, M., Tellmann, S., Burrows, J. P., and Loyola, D.: Ozone profile retrieval from Global Ozone Monitoring Experiment (GOME) data using a neural network approach (Neural Network Ozone Retrieval System (NNORSY)), J. Geophys. Res., 108, 4497, doi:10.1029/2002JD002784, 2003.

Pacifici, F., Chini, M., and Emery, W. J.: A neural network approach using multi-scale textural metrics from very high resolution panchromatic imagery for urban land-use classification, Remote Sens. Environ., 113, 1276–1292, 2009.

Picchiani, M., Chini, M., Corradini, S., Merucci, L., Sellitto, P., Del Frate, F., and Stramondo, S.: Volcanic ash detection and retrievals using MODIS data by means of neural networks, Atmos. Meas. Tech., 4, 2619–2631, doi:10.5194/amt-4-2619-2011, 2011.

Picchiani, M., Del Frate, F., Piscini, A., Chini, M., Corradini, S., Merucci, L., and Stramondo, S.: Associative memory techniques for the exploitation of remote sensing data in the monitoring of volcanic events, in: IEEE International Geoscience and Remote Sensing Symposium (IGARSS), 7298–7301, 2012a.

Picchiani, M., Del Frate, F., Schiavon, G., and Stramondo, S.: Features extraction from SAR interferograms for tectonic applications, EURASIP J. Adv. Sig. Pr., 1, 1–13, 2012b.

Pollack, J. B.,Toon, O. B., and Khare, B. N.: Optical properties of some terrestrial rocks and glasses, Proc. Icarus, 19, 372–389, doi:10.1016/0019-1035(73)90115-2, 1973.

Prata, A. J.: Observations of volcanic ash clouds in the 10–12 mm window using AVHRR/2 data, Int. J. Remote Sens., 10, 751–761, 1989a.

Prata, A. J.: Infrared radiative transfer calculations for volcanic ash clouds, Geophys. Res. Lett., 16, 1293–1296, 1989b.

Prata, A. J. and Kerkmann, J.: Simultaneous retrieval of volcanic ash and SO_2 using MSG-SEVIRI measurements, Geophys. Res. Lett., 34, L05813, doi:10.1029/2006GL028691, 2007.

Pugnaghi, S., Gangale, G., Corradini, S., and Buongiorno, M. F.: Mt. Etna sulfur dioxide flux monitoring using ASTER-TIR data and atmospheric observations, J. Volcanol. Geoth. Res., 152, 74–90, 2006.

Discussion Paper | Discussion Paper | Discussion Paper | Discussion Paper |

AMTD

7, 3349–3395, 2014

Monitoring of volcanic ash and SO_2 from MODIS using Neural Networks

A. Piscini et al.

Title Page

Abstract | Introduction

Conclusions | References

Tables | Figures

◀| |▶

◀ ▶

Back | Close

Full Screen / Esc

Printer-friendly Version

Interactive Discussion

Realmuto, V. J., Abrams, M. J., Buongiorno, M. F., and Pieri, D. C.: The use of multispectral thermal infrared image data to estimate the sulfur dioxide flux from volcanoes: a case study from Mount Etna, Sicily, July 29, 1986, J. Geophys. Res., 99, 481–488, 1994.

Realmuto, V. J., Sutton, A. J., and Elias, T.: Multispectral thermal infrared mapping of sulfur dioxide plumes: a case study from the East Rift Zone of Kilauea Volcano, Hawaii, J. Geophys. Res., 102, 15057–15072, 1997.

Robock, A.: Volcanic eruptions and climate, Rev. Geophys., 38, 191–219, 2000.

Salerno, G. G., Burton, M. R., Oppenheimer, C., Caltabiano, T., Randazzo, D., Bruno, N., and Longo, V.: Three-years of SO_2 flux measurements of Mt. Etna using an automated UV scanner. J. Volcanol. Geotherm. Res., 183, 76–83, doi:10.1016/j.jvolgeores.2009.02.013, 2009.

Sietsma, J. and Dow, R. J.: Neural net pruning-why and how, in: IEEE International Conference on Neural Networks, July 1988, 325–333, 1988.

Sigmundsson, F., Hreinsdóttir, S., Hooper, A., Árnadóttir, T., Pedersen, R., Roberts, M. J., Óskarsson, N., Auriac, A., Decriem, J., Einarsson, P., Geirsson, H., Hensch, M., Ófeigsson, B. G., Sturkell, E., Sveinbjörnsson, H., and Feigl, K. L.: Intrusion triggering of the 2010 Eyjafjallajökull explosive eruption, Nature, 468, 426–430, doi:10.1038/nature09558, 2010.

Sellitto, P., Bojkov, B. R., Liu, X., Chance, K., and Del Frate, F.: Tropospheric ozone column retrieval at northern mid-latitudes from the Ozone Monitoring Instrument by means of a neural network algorithm, Atmos. Meas. Tech., 4, 2375–2388, doi:10.5194/amt-4-2375-2011, 2011.

Smithsonian Institution, Global Volcanism Program, available at: http://www.volcano.si.edu (last access: 20 January 2014), 2014.

Stork, D. and Hassibi, B.: Second order derivatives for network pruning: optimal brain surgeon, in: Advances in Neural Information Processing Systems (NIPS), edited by: Sejnowski, T. J., Hinton, G. E., and Touretzky, D. S., 5th Edn., Morgan Kaufmann Publishers Inc., San Mateo, 164–171, 1993.

Tupper, A., Carn, S., Davey, J., Kamada, Y., Potts, R., Prata, F., and Tokuno, M.: An evaluation of volcanic cloud detection techniques during recent significant eruptions in the western “Ring of Fire”, Remote Sens. Environ., 91, 27–46, 2004.

Wallace, P.: Volcanic SO_2 emissions and the abundance and distribution of exsolved gas in magmas, J. Volcanol. Geotherm. Res., 108, 85–106, 2001.

Watson, I. M., Realmuto, V. J., Rose, W. I., Prata, A. J., Bluth, G. J. S., Gu, Y., Bader, C. E., and Yu, T.: Thermal infrared remote sensing of volcanic emissions using the moderate resolution imaging spectroradiometer, J. Volcanol. Geoth. Res., 135, 75–89, 2004.

AMTD

7, 3349–3395, 2014

Wen, S. and Rose, W. I.: Retrieval of sizes and total masses of particles in volcanic clouds using AVHRR bands 4 and 5, J. Geophys. Res., 99, 5421–5431, 1994.
Yu, T., Rose, W. I., and Prata, A.: Atmospheric correction for satellite-based volcanic ash mapping and retrievals using "split window" IR data from GOES and AVHRR, J. Geophys. Res., 107, 4311, doi:10.1029/2001JD000706, 2002.
Zehner, C.: Editor: Monitoring Volcanic Ash from Space, Proceedings of the ESA-EUMETSAT workshop on the 14 April to 23 May 2010 eruption at the Eyjafjoll volcano, South Iceland, ESA-Publication STM-280, Frascati, Italy, 26–27 May 2010, doi:10.5270/atmch-10-01, 2010.

AMTD
7, 3349–3395, 2014

Monitoring of volcanic ash and SO_2 from MODIS using Neural Networks

A. Piscini et al.

Table 1. MODIS TIR channels characteristics.

Channel no	Center wavelenght (µm)	NEDT (K)	Spatial resolution (km)
28	7.3	0.25	1
29	8.5	0.05	1
30	9.7	0.25	1
31	11.0	0.05	1
32	12.0	0.05	1

AMTD
7, 3349–3395, 2014

Table 2. Training test, test and validations sets for the ash mass, r_{eff} and AOD retrievals.

Date	TrS	TeS	VaS	Tot
6 May 2010	22 365	10 166	8133	40 664
7 May 2010	14 399	6545	5236	26 180
8 Mat 2010	17 640	8018	6414	32 072
13 May 2010	25 527	11 603	9283	46 413
Total	79 931	36 332	29 066	

AMTD
7, 3349–3395, 2014

Table 3. Training test, test and validations sets for the SO_2 retrieval's.

Date	TrS	TeS	VaS	Tot
6 May 2010, 11:55 UTC	13 591	6178	4941	24 710
7 May 2010, 14:30 UTC	10 026	4557	3646	18 229
8 May 2010, 13:20 UTC	7036	3198	2559	5172
13 May 2010, 12:00 UTC	21 471	9760	7807	39 038
Total	51 124	17 693	18 953	

AMTD
7, 3349–3395, 2014

Monitoring of volcanic ash and SO_2 from MODIS using Neural Networks

A. Piscini et al.

AMTD
7, 3349–3395, 2014

Table 4. Independent validation sets for ash parameters divided considering the volcanic plume on sea and volcanic plume on clouds.

Date	VaS (Total)	VaS (Sea)	VaS (Clouds)
11 May 2010, 14:05 UTC	19 640	17 264	2376
12 May 2010, 12:55 UTC	8187	5095	3092

Table 5. Independent SO_2 validation sets for divided into volcanic plume on sea and volcanic plume on clouds.

Date	VaS (Total)	VaS (Sea)	VaS (Clouds)
11 May 2010, 14:05 UTC	13 952	13 754	198
12 May 2010, 12:55 UTC	6211	4343	1868

AMTD
7, 3349–3395, 2014

Table 6. RMSE values related to ash parameters and SO_2 for the independent Validation's sets. The inputs for the ash parameters are the MODIS channels 28-31-32, while for the SO_2 are the MODIS channels 29-31-32.

3 input NN	11 May 2010			12 May 2010		
	Total (std/RMSE)	Sea (std/RMSE)	Clouds (std/RMSE)	Total (std/RMSE)	Sea (std/RMSE)	Clouds (std/RMSE)
Ash Mass	2.29/1.86	2.37/1.96	1.28/0.9	3.32/1.78	3.81/2.16	1.92/0.83
Ash Re	1.44/1.01	1.31/1.02	1.30/0.88	1.54/1.38	1.60/1.41	1.43/1.32
Ash AOD	0.27/0.22	0.27/0.23	0.14/0.09	0.47/0.14	0.39/0.13	0.26/0.15
SO_2	1.61/1.16	1.61/1.15	0.56/1.48	2.03/1.24	2.19/0.79	1.16/1.16

AMTD
7, 3349–3395, 2014

Monitoring of volcanic ash and SO_2 from MODIS using Neural Networks

A. Piscini et al.

Table 7. RMSE values related to ash parameters and SO_2 for the independent Validation's sets.

28 input NN	11 May 2010			12 May 2010		
	Total (std/RMSE)	Sea (std/RMSE)	Clouds (std/RMSE)	Total (std/RMSE)	Sea (std/RMSE)	Clouds (std/RMSE)
Ash Mass	2.29/1.73	2.37/1.78	1.28/1.33	3.32/1.37	3.81/1.44	1.92/1.24
Ash Re	1.44/0.84	1.31/0.39	1.30/2.17	1.54/0.73	1.60/0.24	1.43/1.15
Ash AOD	0.27/0.13	0.27/0.11	0.14/0.24	0.35/0.16	0.39/0.16	0.26/0.15
SO_2	1.61/1.38	1.61/1.34	0.56/3.09	2.04/1.37	2.19/0.75	1.16/2.22

AMTD
7, 3349–3395, 2014

Table 8. RMSE values related to ash parameters and SO_2 for the independent Validation's sets.

Pruned NN	11 May 2010			12 May 2010		
	Total (std/RMSE)	Sea (std/RMSE)	Clouds (std/RMSE)	Total (std/RMSE)	Sea (std/RMSE)	Clouds (std/RMSE)
Ash Mass	2.29/1.36	2.37/1.37	1.28/1.33	3.32/1.31	3.81/1.14	1.92/1.54
Ash Re	1.44/0.91	1.31/0.66	1.30/1.94	1.54/0.83	1.60/0.39	1.43/1.25
Ash AOD	0.35/0.18	0.35/0.18	0.19/0.15	0.47/0.20	0.51/0.20	0.34/0.19
SO_2	1.61/1.42	1.61/1.31	0.56/4.88	2.03/2.00	2.19/1.19	1.16/3.17

AMTD
7, 3349–3395, 2014

Monitoring of volcanic ash and SO_2 from MODIS using Neural Networks

A. Piscini et al.

Table 9. MODIS channels selected by the input pruning.

MODIS Channels	central wavelength [µm]	Parameters			
		AshMass	r_{eff}	AOD	SO_2
1	0.645	×	×	×	
2	0.858		×	×	
3	0.469	×	×	×	×
4	0.555	×	×	×	×
5	1.240	×			
6	1.640	×			×
7	2.130	×	×		
8	0.421	×	×	×	×
17	0.905		×	×	
18	0.936	×	×		
19	0.940	×	×		
20	3.750	×	×		
21	3.959				
22	3.959				×
23	4.050	×	×	×	×
24	4.465				
25	4.515	×	×	×	
26	1.375	×	×		×
27	6.715				
28	7.325				
29	8.550	×		×	×
30	9.730				
31	11.03	×	×	×	×
32	12.02	×	×	×	
33	13.335				
34	13.635				
35	13.935		×		
36	14.235	×	×	×	×
Tot		17	17	12	10

AMTD
7, 3349–3395, 2014

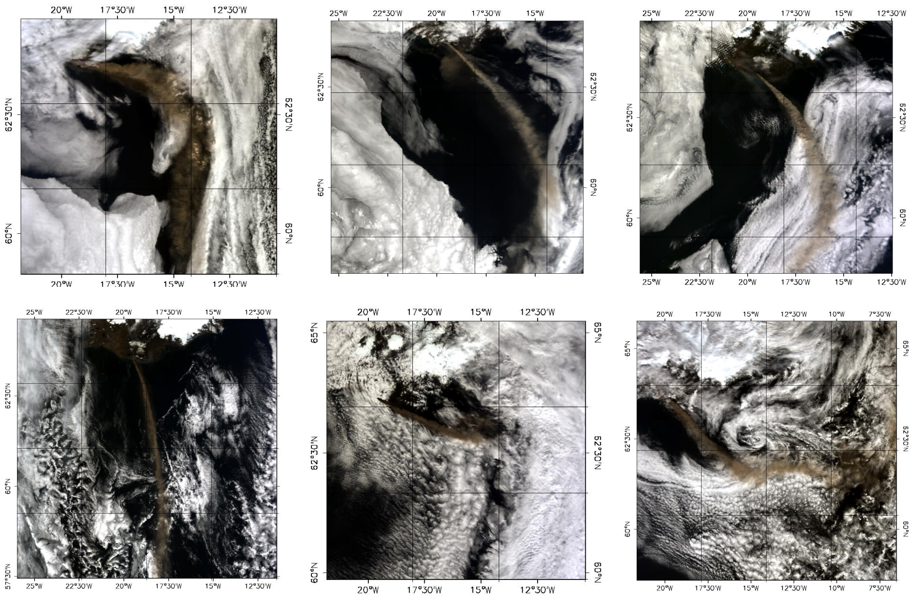

Fig. 1. Six MODIS images RGB (R = ch1, G = ch4, B = ch3), used in this study. (Top) From left to right: 6 May 2010, 11:55 UTC; 7 May 2010, 14:30 UTC; 8 May 2010, 13:20 UTC. (Bottom) From left to right: 11 May 2010, 14:05, UTC; 12 May 2010, 12:55 UTC; 13 May 2010, 12:00 UTC.

AMTD
7, 3349–3395, 2014

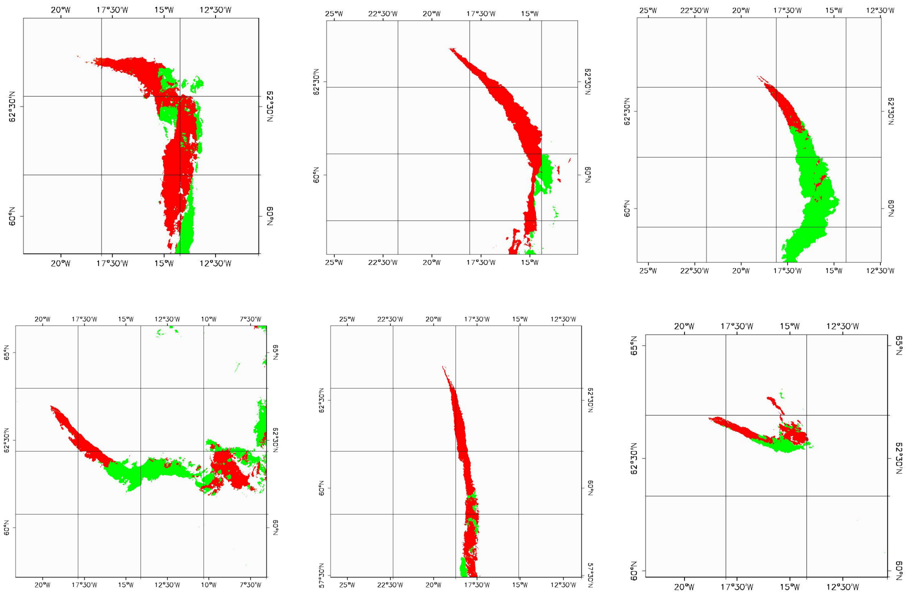

Fig. 2. Ash detection maps of training data-sets: 6 May 2010, 11:55 UTC (top left); 7 May 2010, 14:30 UTC (top middle); 8 May 2010, 13:20 UTC (top right); 13 May 2010, 12:00 UTC (bottom left). The last two images, 11 May 2010, 14:05 UTC (bottom middle) and 12 May 2010, 12:55 UTC (bottom right), represent the validation data-sets. Volcanic ash laying on sea in red colour, on meteorological cloud in green colour, respectively.

AMTD
7, 3349–3395, 2014

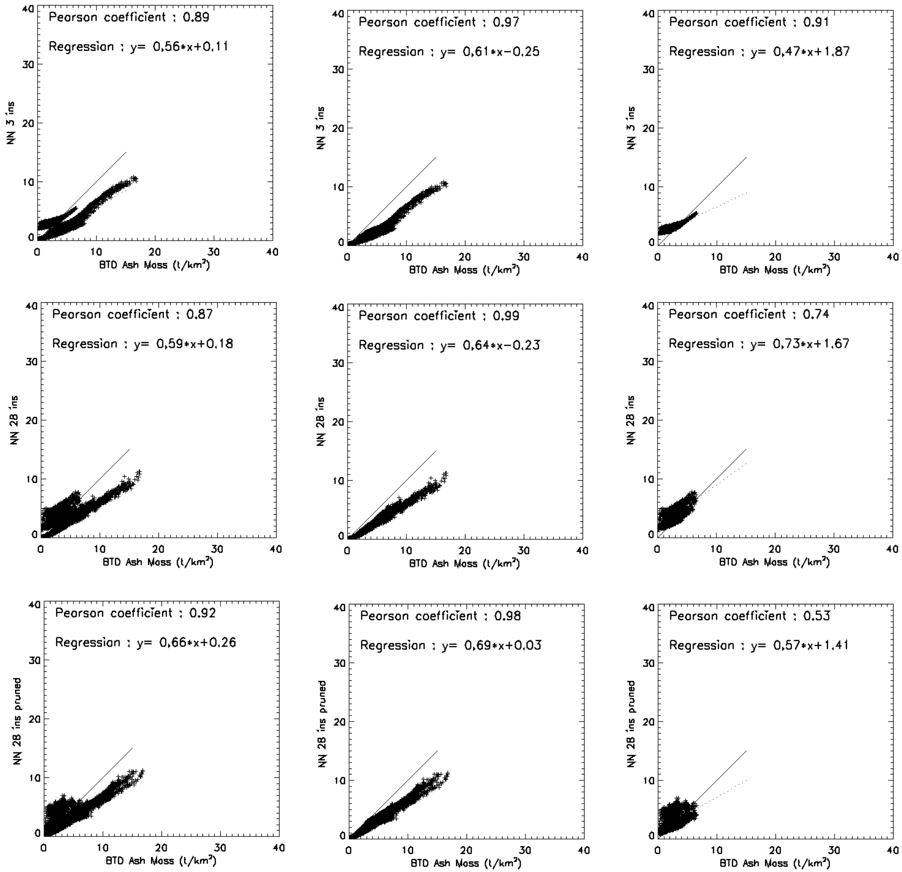

Fig. 3. Scatter plots for ash mass networks, 3 (top row), 28 (middle row) and 28 inputs pruned (bottom row), applied to the validation set of 11 May 2010, 14:05 UTC, divided in total pattern (left column), pattern over sea (middle column), patterns over meteorological cloud (right column).

AMTD
7, 3349–3395, 2014

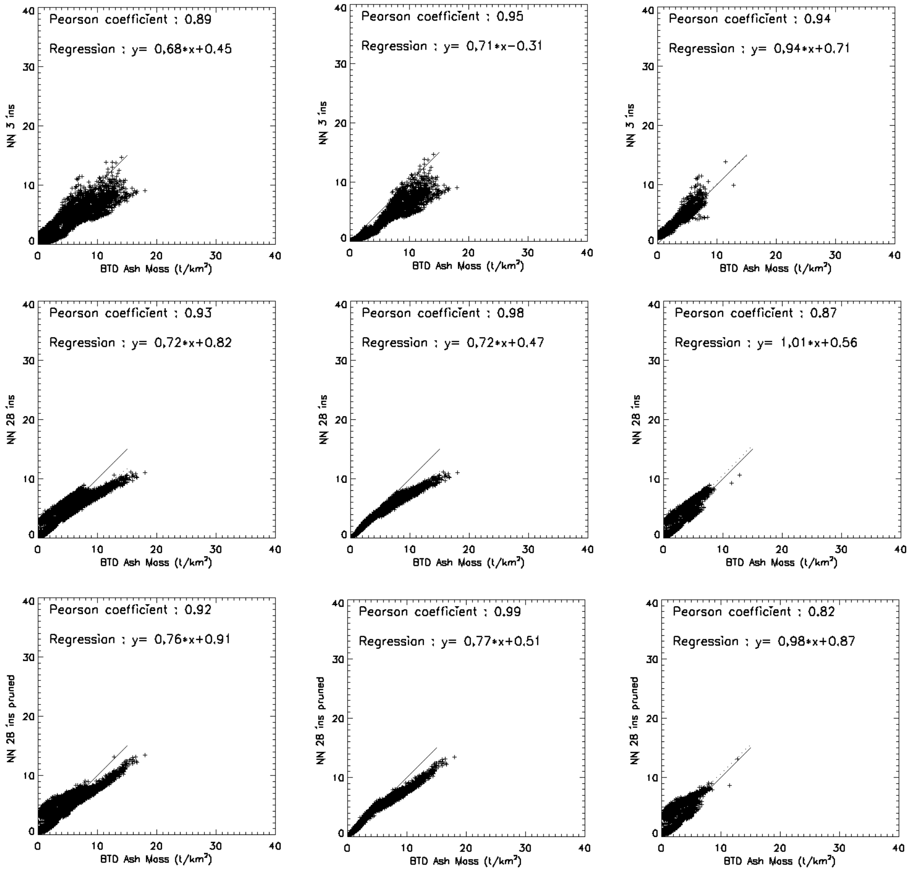

Fig. 4. Scatter plots for ash mass networks, 3 (top row), 28 (middle row) and 28 inputs pruned (bottom) row, applied to the validation set of 12 May 2010, 12:55 UTC, divided in total pattern (left column), pattern over sea (middle column), patterns over meteorological cloud (right column).

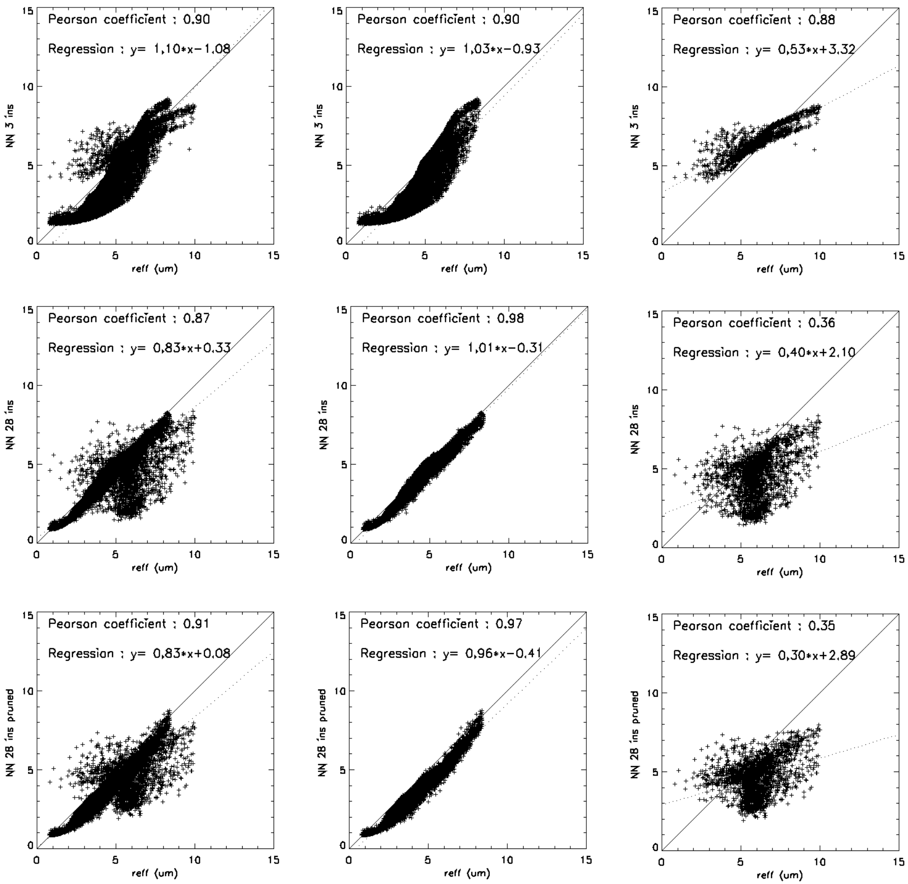

Fig. 5. Scatter plots for r_{eff} networks, 3 (top row), 28 (middle row) and 28 inputs pruned (bottom row), applied to the validation set of 11 May 2010, 14:05 UTC, divided in total pattern (left column), pattern over sea (middle column), patterns over meteorological cloud (right column).

AMTD
7, 3349–3395, 2014

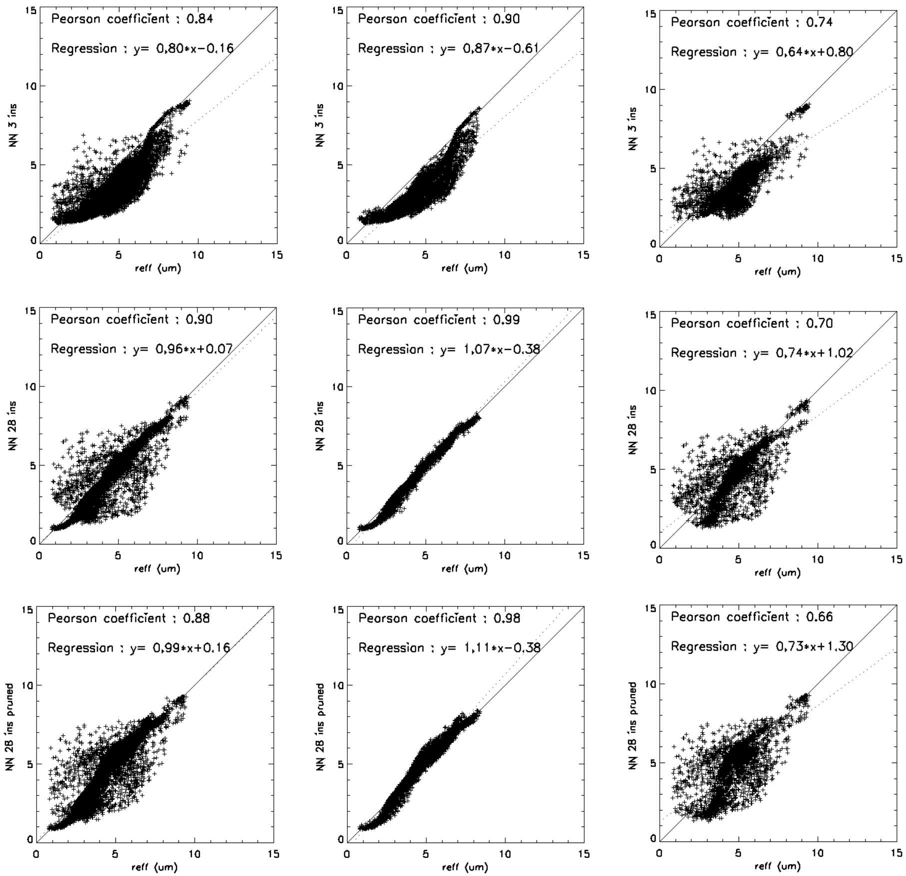

Fig. 6. Scatter plots for reff networks, 3 (top row), 28 (middle row) and 28 inputs pruned (bottom row), applied to the validation set of 12 May 2010, 12:55 UTC, divided in total pattern (left column), pattern over sea (middle column), patterns over meteorological cloud (right column).

AMTD
7, 3349–3395, 2014

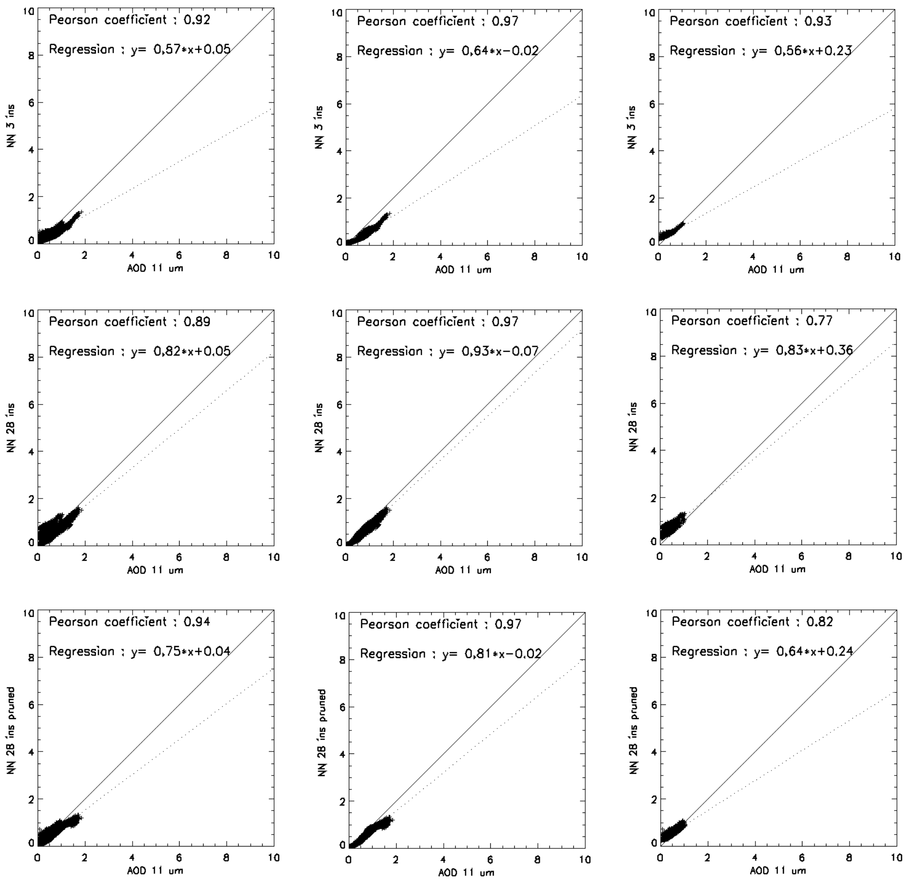

Fig. 7. Scatter plots for AOD networks, 3 (top row), 28 (middle row) and 28 inputs pruned (bottom row), applied to the validation set of 11 May 2010, 14:05 UTC, divided in total pattern (left column), pattern over sea (middle column), patterns over meteorological cloud (right column).

AMTD
7, 3349–3395, 2014

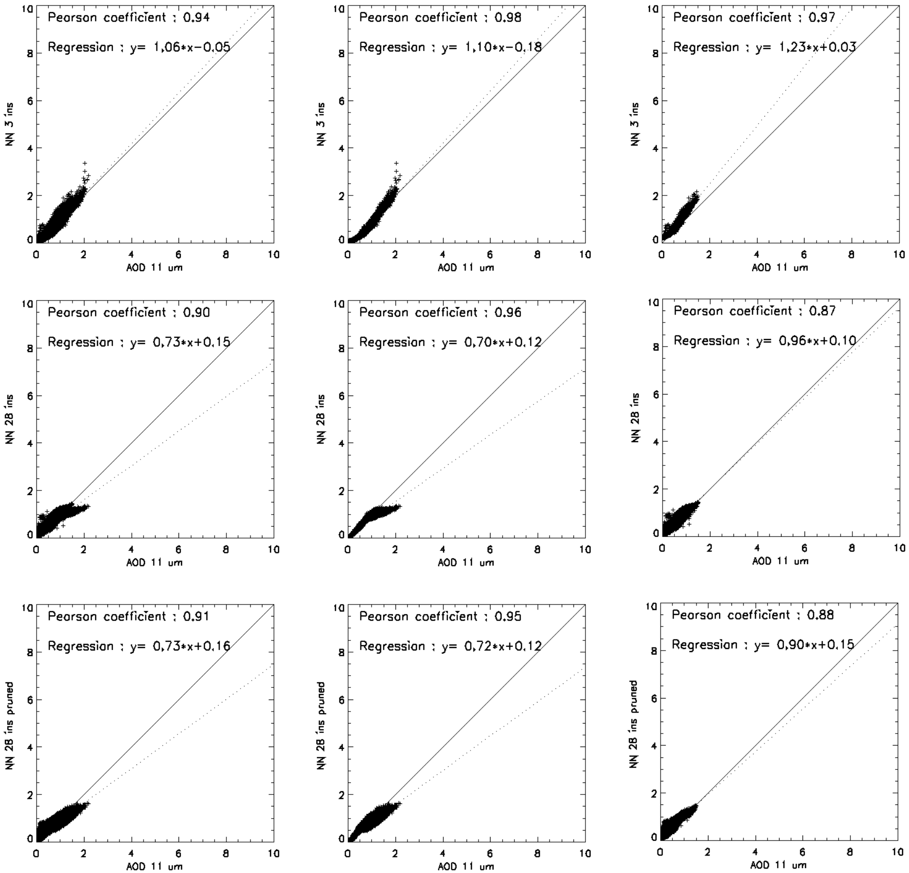

Fig. 8. Scatter plots for AOD networks, 3 (top row), 28 (middle row) and 28 inputs pruned (bottom row), applied to the validation set of 12 May 2010, 12:55 UTC, divided in total pattern (left column), pattern over sea (middle column), patterns over meteorological cloud (right column).

AMTD
7, 3349–3395, 2014

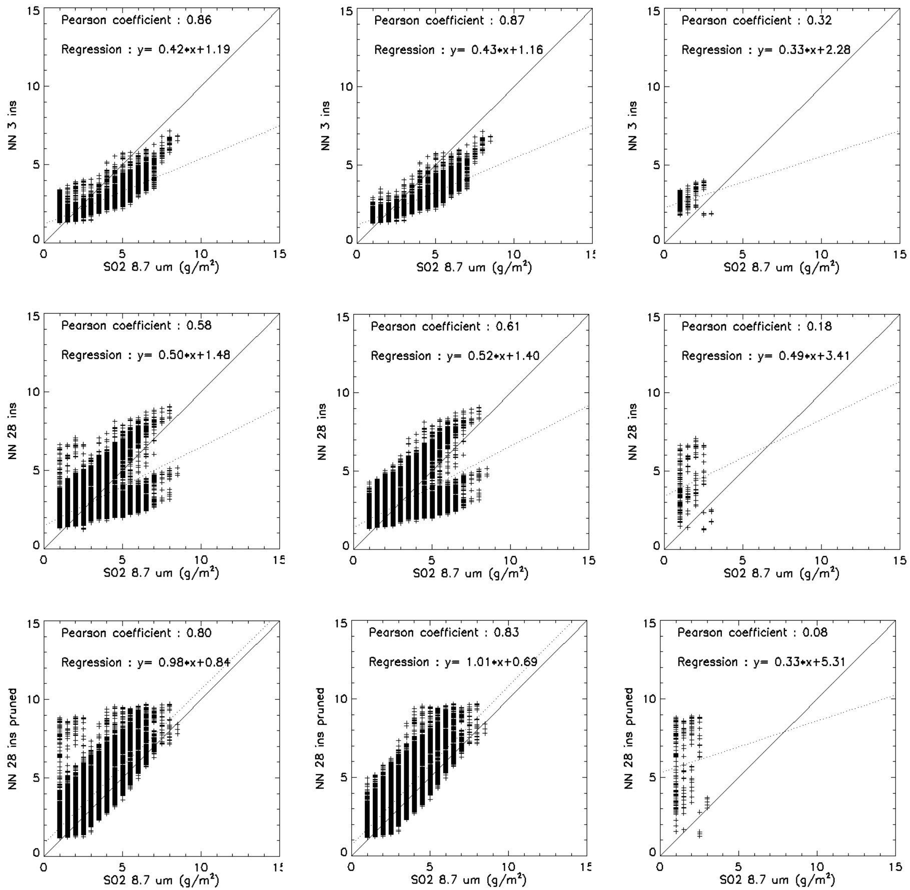

Fig. 9. Scatter plots for SO_2 networks, 3 (top row), 28 (middle row) and 28 inputs pruned (bottom row), applied to the validation set of 11 May 2010, 14:05 UTC, divided in total pattern (left column), pattern over sea (middle column), patterns over meteorological cloud (right column).

AMTD
7, 3349–3395, 2014

Monitoring of volcanic ash and SO_2 from MODIS using Neural Networks

A. Piscini et al.

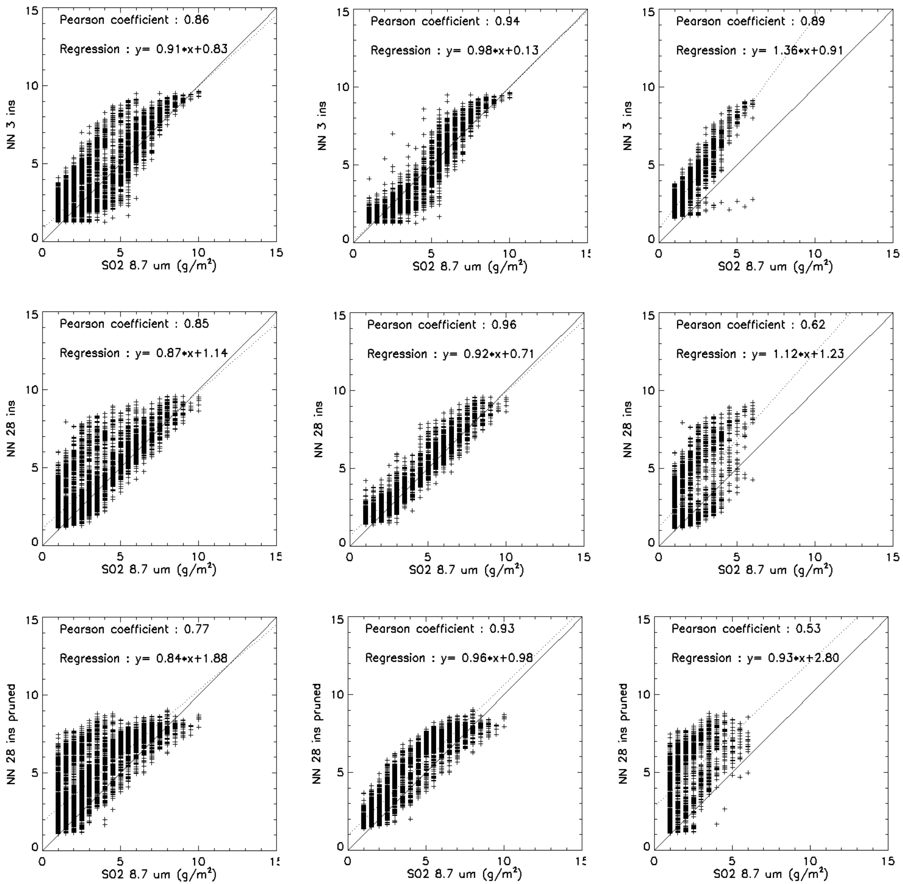

Fig. 10. Scatter plots for SO_2 networks, 3 (top row), 28 (middle row) and 28 inputs pruned (bottom row), applied to the validation set of 12 May 2010, 12:55 UTC, divided in total pattern (left column), pattern over sea (middle column), patterns over meteorological cloud (right column).

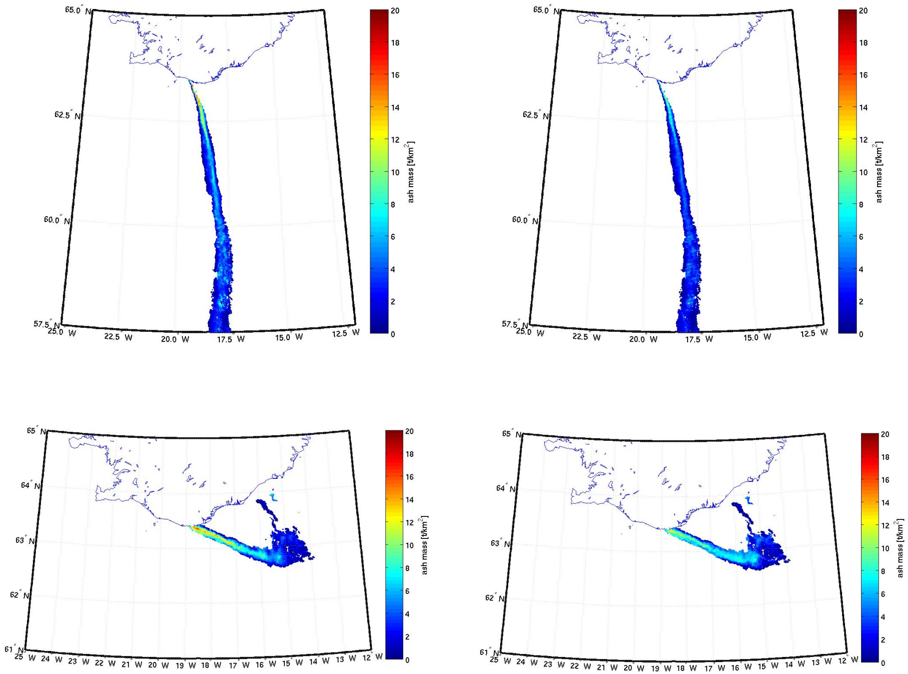

Fig. 11. Ash mass maps: top 11 May 2010, bottom 12 May 2010. Left: target retrieval, right: retrieval from pruned neural network.

AMTD
7, 3349–3395, 2014

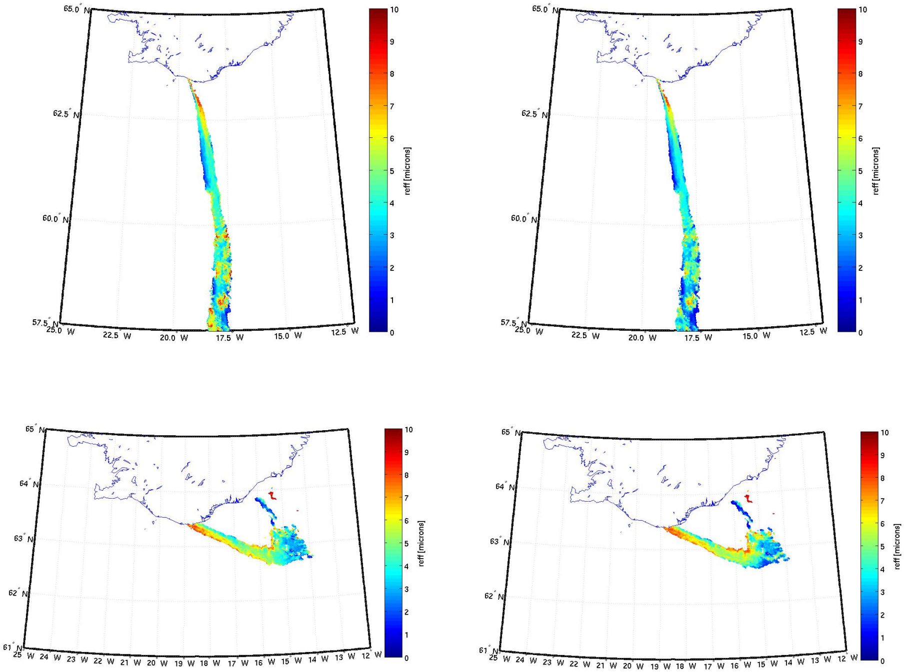

Fig. 12. r_{eff} maps. Top: 11 May 2010; bottom: 12 May 2010. Left: target retrieval; right: retrieval from pruned neural network.

AMTD

7, 3349–3395, 2014

Monitoring of volcanic ash and SO_2 from MODIS using Neural Networks

A. Piscini et al.

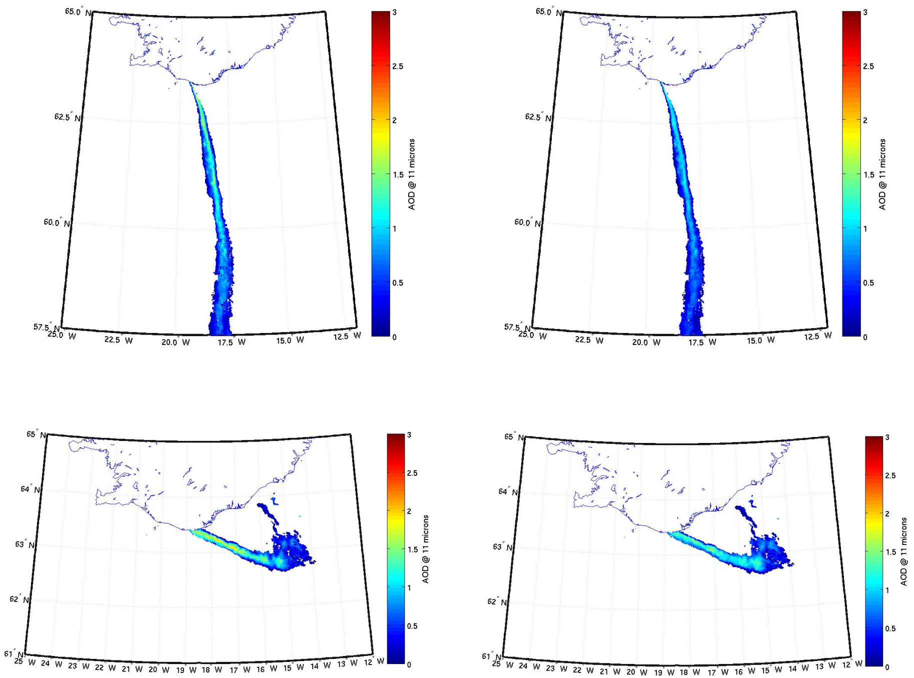

Fig. 13. AOD maps. Top: 11 May 2010; bottom: 12 May 2010. Left: target retrieval; right: retrieval from pruned neural network.

AMTD

7, 3349–3395, 2014

Monitoring of volcanic ash and SO_2 from MODIS using Neural Networks

A. Piscini et al.

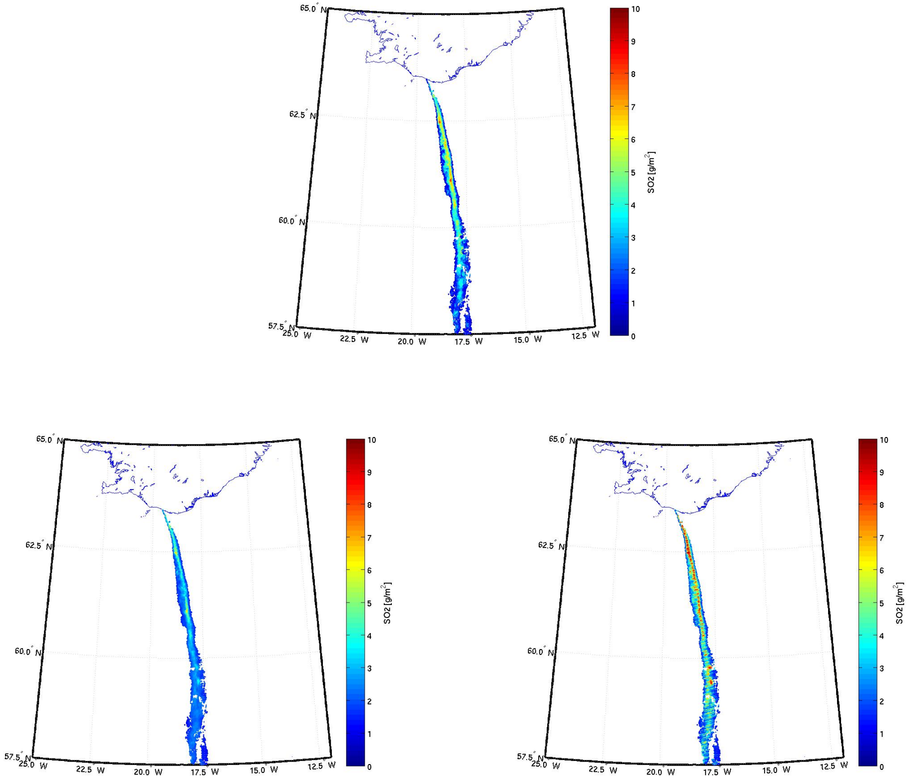

Fig. 14. SO_2 columnar abundance maps for 11 May 2010. Top: target retrieval; bottom left: retrieval from 3 inputs neural network; bottom right: retrieval from pruned neural network.

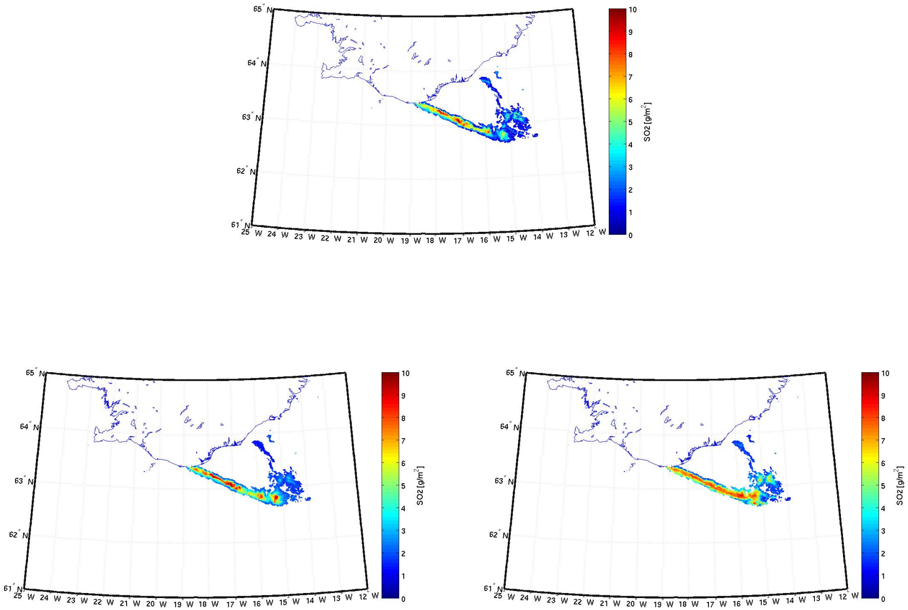

Fig. 15. SO_2 columnar abundance maps for 12 May 2010. Top: target retrieval; bottom left: retrieval from 3 inputs neural network; bottom right: retrieval from pruned neural network.

AMTD

7, 3349–3395, 2014

Monitoring of volcanic ash and SO_2 from MODIS using Neural Networks

A. Piscini et al.